

Temperature effect on U(VI) sorption onto Na-bentonite

Z. Yang, L. Huang, Z. Guo, Gilles Montavon, W. Wu

► **To cite this version:**

Z. Yang, L. Huang, Z. Guo, Gilles Montavon, W. Wu. Temperature effect on U(VI) sorption onto Na-bentonite. *Radiochimica Acta*, R Oldenbourg Verlag GMBH, 2010, 98, pp.785-791. 10.1524/ract.2010.1784 . in2p3-00611649

HAL Id: in2p3-00611649

<http://hal.in2p3.fr/in2p3-00611649>

Submitted on 26 Jul 2011

HAL is a multi-disciplinary open access archive for the deposit and dissemination of scientific research documents, whether they are published or not. The documents may come from teaching and research institutions in France or abroad, or from public or private research centers.

L'archive ouverte pluridisciplinaire **HAL**, est destinée au dépôt et à la diffusion de documents scientifiques de niveau recherche, publiés ou non, émanant des établissements d'enseignement et de recherche français ou étrangers, des laboratoires publics ou privés.

1 **Temperature effect on U(VI) sorption onto Na-bentonite**

2 *Ziqian Yang^a, Lei Huang^a, Zhijun Guo^{a,*}, Gilles Montavon^b, Wangsuo Wu^a*

3 ^aRadiochemistry Lab, School of Nuclear Science and Technology, Lanzhou
4 University, 730000, Lanzhou, China

5 ^bSubatech Laboratory, CNRS/In2P3/Ecole des Mines de Nantes/Université de
6 Nantes, 4 rue Alfred Kastler, BP 20722, 44307 Nantes, France

7 *Sorption / U(VI) / Na-bentonite / Temperature effect / Surface complexation model*

8 **Summary**

9 U(VI) sorption on a purified Na-bentonite was investigated from 298±2 to 353±2 K
10 by using a batch experimental method as a function of pH, U(VI) concentration,
11 carbonate concentration and solid-to-liquid ratio (*m/V*). The data at 298±2 K could
12 be well described by a surface complexation model (SCM) with a complex located
13 on layer sites (X_2UO_2) and three complexes located on edge sites ($\equiv SOUO_2^+$,
14 $\equiv SO(UO_2)_3(OH)_5$, and $\equiv SO(UO_2)_3(OH)_7^{2-}$). The intrinsic equilibrium constants (K^{int})
15 of the surface reactions at 333±2 K and 353±2 K were obtained by fitting U(VI)
16 sorption curves versus pH on the Na-bentonite. The model enables U(VI) sorption in
17 the presence of carbonate ($P_{CO_2} = 10^{-3.58}$ atm) to be described without considering any
18 ternary surface complexes involving carbonate, except for underestimation around
19 pH 7 ($6 < \text{pH} < 7.5$). The standard enthalpy changes ($\Delta_r H_m^\theta$) of the surface reactions
20 were evaluated from the K^{int} values obtained at three temperatures (298±2, 333±2

* Corresponding author, E-mail address: guozhj@lzu.edu.cn (Z. GUO)

1 and 353 ± 2 K) via the van't Hoff equation. The proposed SCM and $\Delta_r H_m^\circ$ of the
2 surface reactions enable U(VI) sorption on the Na-bentonite at other temperatures to
3 be predicted.

4 **1. Introduction**

5 Because of its excellent physicochemical properties such as high specific surface
6 area, large cation exchange and sorption capacity, and good swelling and sealing
7 nature, bentonite has been considered as a backfilling material for deep geological
8 repository of high-level radioactive waste in many countries. Uranium(VI) is an
9 important contaminant to be considered in nuclear waste management and the
10 sorption of U(VI) on bentonite/montmorillonite has received special attentions [1-9].
11 Different surface complexation models (SCMs) have been proposed to quantitatively
12 describe macroscopic sorption of U(VI) on bentonite/montmorillonite using two
13 main approaches. The first one treats montmorillonite as an aggregate of
14 fixed-charge sites and edge sites analogous to gibbsite and silica [1]. The surface
15 complexation constants for uranyl binding to gibbsite and silica were used for the
16 edge sites. Different electrostatic models were chosen, for example, a triple-layer
17 model was used by Turner et al. [2], whereas a constant capacitance model was used
18 by Kowal-Fouchard et al [6]. Another approach is to consider montmorillonite as a
19 specific sorbent. The capacity of layer sites is estimated by CEC measurement, while
20 the densities of edge sites as well as the protonation and deprotonation constants are
21 obtained by fitting the acid-base titration data at variable ionic strengths [10-14].

1 It is well known that the near-field temperature in deep geological repository for
2 high-level radioactive waste may be higher than the ambient temperature and vary
3 with time because of radionuclide decay [15-17]. However, most sorption data
4 reported up to date were collected at ambient temperature and studies on temperature
5 effect are still lacking [15]. In this paper, U(VI) sorption on a purified Na-bentonite at
6 298 ± 2 K was studied as a function of pH, U(VI) concentration, solid-to-liquid ratio
7 (m/V) and carbonate concentration by batch sorption experiments, and a SCM was
8 constructed based on the sorption data collected at 298 ± 2 K. Then, U(VI) sorption
9 curves versus pH on the Na-bentonite at elevated temperatures (333 ± 2 K and 353 ± 2 K)
10 were collected and the proposed SCM was fitted to these sorption data at elevated
11 temperatures, respectively, to obtain the intrinsic equilibrium constants (K^{int}) of the
12 surface complexation reactions at elevated temperatures. Finally, the K^{int} at three
13 temperatures (298 ± 2 , 333 ± 2 and 353 ± 2 K) were used to assess $\Delta_r H_m^\circ$ of the surface
14 complexation reactions via the van't Hoff equation.

15 **2. Experimental**

16 **2.1 Materials**

17 The Na-bentonite used in this work was obtained from Jinchuan Bentonite Company
18 (Jinchuan, Gansu Province, China). The protocols of purification and
19 characterization of the purified Na-bentonite have been described in our previous
20 paper [14]. The purified Na-bentonite is mainly composed of 12 wt.% quartz and 88
21 wt.% montmorillonite with a calculated structural formula of $[\text{Si(IV)}_8](\text{Al(III)}_{3.19},$

1 Fe(III)_{0.29}, Fe(II)_{0.38},Mg(II)_{0.14})O₂₀(OH)₄(Ca(II)_{0.023},Na(I)_{0.35},K(I)_{0.127}). The CEC was
2 experimentally found to be 623±12 meq/kg and is consistent with the value
3 calculated according to the structural formula. The specific surface area obtained by
4 B.E.T. analyses using N₂ was found to be 53.6 m²/g. A uranium(VI) stock solution
5 was prepared from UO₂(NO₃)₂·6H₂O (A.R. grade, made in China). All other
6 chemicals used were at least analytical grade. All solutions were prepared with
7 deionized water (18MΩ/cm).

8 **2.2 Sorption**

9 Sorption experiments were carried out in a nitrogen atmosphere glove box, except
10 for the sorption in the presence of carbonate. The Na-bentonite was dispersed with
11 NaCl solution (0.1mol/L) in polyethylene tubes and the pH of the suspension was
12 adjusted by adding small amounts of HCl or NaOH solutions. Proper amounts of the
13 uranium stock solution were added and the suspension was shaken for 2 days before
14 analysis. The elevated temperature was controlled by a water bath. Our prior
15 sorption experiments demonstrated that sorption steady state can be reached within 2
16 days. The pH of the suspension was recorded at the experimental temperature on a
17 Metrohm 781 pH/ion Meter with a combined glass electrode (Metrohm
18 No.6.0234.100) which was calibrated with three standard buffers. Phase separation
19 was carried out by centrifugation at 18000g for 30 min. The concentration of U(VI)
20 in the aqueous phase was analyzed by spectrophotometry at a wavelength of 652 nm
21 by using U(VI) and Arsenazo-III complex. The relative errors of spectrophotometric
22 measurements were less than 5%. The sorption on the tube walls was negligible. The

1 amount of U(VI) sorbed (q , mol/g) was calculated by the difference of the initial and
2 final concentrations in the aqueous phase (C_0 and C_{eq} , respectively, mol/L):

$$3 \quad q = \frac{V}{m}(C_0 - C_{eq}) \quad (1)$$

4 where V (L) is the volume of aqueous phase and m (g) the mass of Na-bentonite. The
5 sorption percentage of U(VI) was calculated by

$$6 \quad \text{Sorption (\%)} = \frac{C_0 - C_{eq}}{C_0} \times 100 . \quad (2)$$

7 The sorption experiment in the presence of carbonate was performed at the normal
8 atmospheric condition ($P_{CO_2} = 10^{-3.58}$ atm). The pH of Na-bentonite suspension was
9 adjusted with HCl or $NaHCO_3/Na_2CO_3$ solutions. The tubes were opened regularly
10 during sorption until the pH values were stable. The analytical methods were the
11 same as described above.

12 **2.3 Modeling**

13 The sorption of U(VI) was interpreted by a double layer model (DLM), based on the
14 acid-base chemistry of the Na-bentonite which has been reported in detail in our
15 previous paper [14]. Two types of sorption sites were considered: layer sites (X^-) and
16 edge sites. Both aluminol ($\equiv SOH$) and silanol ($\equiv YOH$) edge sites were included
17 for the acid-base chemistry of the Na-bentonite. The capacities of the sites as well as
18 the constants of protonation and deprotonation were summarized in Table 1. The
19 code PHREEQC [18] was used for modeling calculations. Activity correction of the
20 aqueous species was made by the Davies equation. U(VI) thermodynamic data used

1 in modeling were taken from the NEA (Nuclear Energy Agency) database [19],
2 except for those of $\text{UO}_2(\text{OH})_2(\text{aq})$ which were taken from the Nagra/PSI Chemical
3 Thermodynamic Data Base [20]; in the NEA database, only a maximum limit of the
4 equilibrium constant was given for this species. The U(VI) thermodynamic data used
5 in the modeling are listed in Table 2.

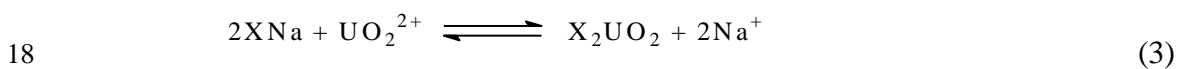
6 **3. Results and Discussion**

7 **3.1 U(VI) sorption on Na-bentonite at $T = 298 \pm 2$ K**

8 Sorption curves of U(VI) versus pH on the Na-bentonite at 298 ± 2 K and different
9 U(VI) concentrations (4.01×10^{-5} and 8.02×10^{-5} mol/L) are presented in Fig. 1. The
10 sorption of U(VI) on Na-bentonite is strongly pH-dependent; the sorption percentage
11 of U(VI) increases slightly up to pH 4 and then increases significantly in the pH
12 range of 4—8. This is consistent with previous observations of U(VI) sorption on
13 montmorillonite/bentonite [2, 6]. The sorption curve of U(VI) versus pH at 8.02×10^{-5}
14 mol/L is shifted somewhat to higher pH in comparison with that at 4.01×10^{-5} mol/L,
15 indicating that U(VI) sorption percentage decreases with U(VI) concentration at a
16 given pH. The inflection of sorption curves of U(VI) against pH results from a
17 variation of sorption mechanisms. In the low pH range, U(VI) sorption on
18 bentonite/montmorillonite has been interpreted by cation exchange on layer sites,
19 whereas U(VI) surface complexation reactions on edge sites occur at $\text{pH} > 4$ [3, 6,
20 11]. The two types of U(VI) surface species have been supported by spectroscopic
21 studies. Extended X-ray absorption fine structure (EXAFS) studies on U(VI)

1 sorption on montmorillonite have suggested that U(VI) adsorption on
 2 montmorillonite is most likely through an outer-sphere cation-exchange mechanism
 3 at low pH, whereas a transition to an inner-sphere surface complexation mechanism
 4 occurs at near neutral pH [7-8]. However, the detailed nature of the surface species
 5 formed at the edge sites can not be simply deduced from these spectroscopic studies
 6 [3]. Surface complexes are usually supposed based on analogous speciation in the
 7 aqueous phase [3, 11]. U(VI) speciation in the aqueous phase strongly depends on
 8 experimental conditions such as pH, U(VI) concentration, and the presence of
 9 ligands [21]. For comparison, both U(VI) speciations in the absence and presence of
 10 CO₂ ($P_{CO_2} = 10^{-3.58}$ atm) at $C_{U(VI)}^0 = 4.0 \times 10^{-5}$ mol/L and $I = 0.1$ mol/L NaCl are
 11 shown in Fig. 2. UO₂²⁺ is the dominant species at pH ≤ 5 in both CO₂ conditions and
 12 U(VI) polynuclear hydrolysis products, (UO₂)₃(OH)₅⁺ and (UO₂)₃(OH)₇⁻, become
 13 major species in the high pH range in the absence of CO₂. Therefore, UO₂²⁺,
 14 (UO₂)₃(OH)₅⁺ and (UO₂)₃(OH)₇⁻ are considered as the U(VI) species sorbed at the
 15 surface in the present study.

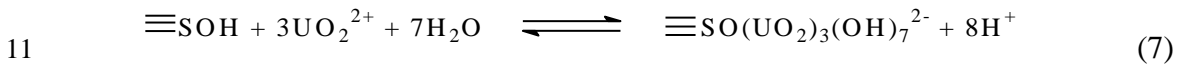
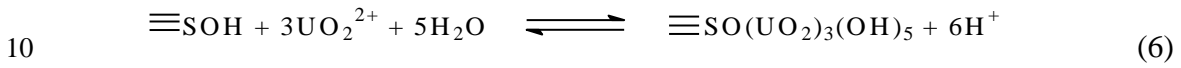
16 The first surface reaction considered in the modeling is the binding of UO₂²⁺ on the
 17 layer sites (X⁻):



$$19 \quad K_1 = \frac{[X_2UO_2][Na^+]^2}{[XNa]^2[UO_2^{2+}]} \cdot \frac{\gamma_{Na^+}^2}{\gamma_{UO_2^{2+}}} \quad (4)$$

20 As expected, U(VI) sorption in the low pH range can be described by reaction (3),
 21 other surface reactions on edge sites must be considered to interpret the sharp

1 increase in the high pH range. Inner-sphere surface complexes of UO_2^{2+} and
 2 $(\text{UO}_2)_3(\text{OH})_5^+$ on both aluminol and silanol edge sites are commonly considered [1-3,
 3 6, 9]. Since aluminol sites are much more reactive than silanol sites [4, 16] and
 4 cations primarily sorb on octahedral sites such as $\text{Al}(\text{O}, \text{OH})_6$ and $\text{Fe}(\text{O}, \text{OH})_6$ [8],
 5 only surface complexation reactions on aluminol sites ($\equiv\text{SOH}$) were considered in
 6 the present paper. Similar modeling strategies have been used to interpret Eu(III)
 7 sorption on montmorillonite/bentonite [14, 16]. Surface complexation reactions of
 8 UO_2^{2+} , $(\text{UO}_2)_3(\text{OH})_5^+$ and $(\text{UO}_2)_3(\text{OH})_7^{2-}$ on $\equiv\text{SOH}$ can be respectively expressed as:



12 The corresponding intrinsic equilibrium constants of reactions (5)–(7) are as
 13 follows:

$$14 \quad K_2^{\text{int}} = \frac{[\equiv\text{SOUO}_2^+][\text{H}^+]}{[\equiv\text{SOH}][\text{UO}_2^{2+}]} \cdot \frac{\gamma_{\text{H}^+}}{\gamma_{\text{UO}_2^{2+}}} \exp(F\Psi / RT) \quad (8)$$

$$15 \quad K_3 = \frac{[\equiv\text{SO}(\text{UO}_2)_3(\text{OH})_5][\text{H}^+]^6}{[\equiv\text{SOH}][\text{UO}_2^{2+}]^3} \cdot \frac{\gamma_{\text{H}^+}^6}{\gamma_{\text{UO}_2^{2+}}^3} \quad (9)$$

$$16 \quad K_4^{\text{int}} = \frac{[\equiv\text{SO}(\text{UO}_2)_3(\text{OH})_7^{2-}][\text{H}^+]^8}{[\equiv\text{SOH}][\text{UO}_2^{2+}]^3} \cdot \frac{\gamma_{\text{H}^+}^8}{\gamma_{\text{UO}_2^{2+}}^3} \exp(-2F\Psi / RT) \quad (10)$$

17 A stepwise fitting approach [11] was used to evaluate the equilibrium constants of
 18 the surface reactions by fitting U(VI) sorption curves versus pH at 298 ± 2 K (Fig. 1).
 19 Surface reactions (3) and (5)–(7) were sequentially considered to describe the

1 sorption curves of U(VI) against pH from low to high pH and finally the equilibrium
2 constants at 298 ± 2 K were estimated (Table 3). The calculated results are shown as
3 lines in Fig. 1.

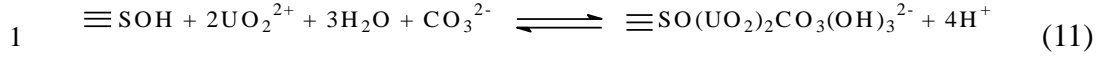
4 The model was then used as a predictive tool to describe experimental data measured
5 as a function of U(VI) concentration and m/V . Two U(VI) sorption isotherms at
6 298 ± 2 K and different pH (4.78 ± 0.10 and 5.76 ± 0.10) were collected (Fig. 3). The
7 two isotherms are almost parallel and are well described by the model. Moreover,
8 U(VI) sorption dependence on m/V was carried out at $T = 298\pm 2$ K, $C_{\text{U(VI)}}^0 =$
9 8.02×10^{-5} mol/L, pH 5.00 ± 0.10 and $I = 0.1$ mol/L NaCl. As seen in Fig. 4, the
10 sorption percentage of U(VI) increases with m/V , due to the increase of available
11 sites, which is well reproduced by the model. The good interpretation for the U(VI)
12 sorption isotherms and the sorption dependence on m/V imply that the proposed
13 model is reasonable.

14 **3.2 U(VI) sorption at $P_{\text{CO}_2} = 10^{-3.58}$ atm and $T = 298\pm 2$ K**

15 Carbonate is an extensive ligand in the environment and the partial pressure of CO_2 in
16 aquifers commonly reaches values of 1—5% [22]. Since carbonate has a strong
17 binding affinity for uranyl, the effect of carbonate on U(VI) sorption is of importance.
18 A sorption curve of U(VI) versus pH on the Na-bentonite in the presence of CO_2
19 ($P_{\text{CO}_2} = 10^{-3.58}$ atm) was also collected in this study to evaluate the effect of carbonate
20 and to test the performance of the proposed model. For comparison, U(VI) sorption
21 data in the absence and presence of CO_2 as a function of pH are simultaneously shown
22 in Fig. 5. At pH < 6.0 , the two series of sorption data are identical, suggesting that in
23 the low pH range the presence of CO_2 has a negligible influence on U(VI) sorption.
24 At pH around 7 ($6 < \text{pH} < 7.5$), U(VI) sorption increases somewhat in the presence of

1 CO₂, whereas at pH > 7.5 U(VI) sorption decreases compared to that in the absence of
 2 CO₂. Since the concentration of carbonate in the aqueous phase increases significantly
 3 with increasing pH at a constant CO₂ partial pressure, the difference between the
 4 sorption curves of U(VI) versus pH in the absence and presence of CO₂ may be
 5 related to an effect of carbonate on U(VI) speciation in the aqueous phase [3, 9]. As
 6 seen in Fig. 2, in the presence of CO₂ ($P_{CO_2} = 10^{-3.58}$ atm), the importance of
 7 (UO₂)₃(OH)₅⁺ in the alkaline pH range is to some extent decreased and the content of
 8 (UO₂)₃(OH)₇⁻ is completely suppressed, due to the formation of (UO₂)₂CO₃(OH)₃⁻,
 9 UO₂(CO₃)₂²⁻ and UO₂(CO₃)₃⁴⁻. Considering that the montmorillonite surface at a pH
 10 near 7 and in alkaline pH region is negatively charged [13, 14], the affinity of high
 11 negatively charged uranyl complexes of carbonate, UO₂(CO₃)₂²⁻ and UO₂(CO₃)₃⁴⁻, for
 12 the surface may be weaker than the U(VI) hydrolysis products, (UO₂)₃(OH)₅⁺ and
 13 (UO₂)₃(OH)₇⁻, because of higher electrostatic repulsion. Thus, the sorption of U(VI)
 14 decreases sharply in the presence of CO₂ at pH > 7.5 compared to that in the absence
 15 of CO₂. This is in agreement with the carbonate effect on U(VI) sorption on other
 16 minerals such as ferrihydrite [23] and hematite [24]. A similar decrease of Eu(III)
 17 sorption on the Na-bentonite was also observed in the presence of CO₂ [14]. The
 18 higher U(VI) sorption around pH 7 (6 < pH < 7.5) in the presence of CO₂ may be due
 19 to the binding of (UO₂)₂CO₃(OH)₃⁻ on the surface because (UO₂)₂CO₃(OH)₃⁻ is the
 20 dominant U(VI) aqueous species around pH 7 in addition to (UO₂)₃(OH)₅⁺.

21 As a first estimation, the proposed model without considering any ternary surface
 22 complexes of carbonate was used to predict the U(VI) sorption curve versus pH in
 23 the presence of CO₂ at $P_{CO_2} = 10^{-3.58}$ atm, $C_{U(VI)}^0 = 8.02 \times 10^{-5}$ mol/L, $I = 0.1$ M NaCl,
 24 and $m/V = 1$ g/L. As can be seen in Fig. 5, the model could readily interpret the
 25 identical sorption at pH < 6 and the lower sorption at pH > 7.5. However, it
 26 underestimates U(VI) sorption around pH 7 (6.0 < pH < 7.5). To improve the
 27 agreement, the binding of (UO₂)₂CO₃(OH)₃⁻ on ≡SOH was considered:



2 Although ternary surface complexes of U(VI) and carbonate on montmorillonite
 3 have been suggested by a recent EXAFS study [8], modeling exercises indicated that
 4 reaction (11) could not improve the fitting goodness for the sorption curve of U(VI)
 5 versus pH in the presence of CO₂ (Fig. 5). The reason is not clear and further
 6 investigation is still needed.

7 **3.3 Effect of temperature on U(VI) sorption onto Na-bentonite**

8 The influence of temperature on chemical reactions can be described by the van't
 9 Hoff equation:

$$10 \quad \log K^\theta = -\frac{\Delta_r H_m^\theta}{2.303 R} \cdot \frac{1}{T} + \frac{\Delta_r S_m^\theta}{2.303 R} \quad (12)$$

11 where K^θ is the standard equilibrium constant of the reaction at absolute temperature
 12 T , R the gas constant, $\Delta_r H_m^\theta$ the standard enthalpy change and $\Delta_r S_m^\theta$ the standard
 13 entropy change. When $\Delta_r H_m^\theta$ and $\Delta_r S_m^\theta$ are considered as constants with
 14 temperature, $\Delta_r H_m^\theta$ can be evaluated by the slope of $\log K^\theta$ against $1/T$ plot. The
 15 relationship between K_1^θ at T_1 and K_2^θ at T_2 can be described by

$$16 \quad \ln\left(\frac{K_2^\theta}{K_1^\theta}\right) = \frac{-\Delta_r H_m^\theta}{R} \left(\frac{1}{T_2} - \frac{1}{T_1}\right) \quad (13)$$

17 With a known $\Delta_r H_m^\theta$ and K_1^θ at T_1 , Eq. (13) can be used to estimate K_2^θ at any
 18 other T_2 . Considering the temporal and spatial variation of temperature in the near
 19 field of deep geological repository for high-level radioactive waste, $\Delta_r H_m^\theta$ of

1 surface reactions involving radionuclide sorption on back-filling materials (e.g.
2 bentonite) are necessary for nuclear waste management [15-17]. In this study, U(VI)
3 sorption curves versus pH on the Na-bentonite measured at $C_{\text{U(VI)}}^0 = 8.02 \times 10^{-5}$
4 mol/L, $I = 0.1 \text{ mol/L NaCl}$, $m/V = 1 \text{ g/L}$ and three temperatures (298 ± 2 , 333 ± 2 and
5 $353 \pm 2 \text{ K}$) were collected to evaluate the $\Delta_r H_m^\theta$ of surface reactions in the proposed
6 model. As shown in Fig. 6, U(VI) sorption on the Na-bentonite does not vary with
7 temperature at $\text{pH} < 3.5$, suggesting that the temperature effect on U(VI) binding to
8 the layer sites is negligible. Above pH 3.5, U(VI) sorption on the solid phase
9 increases with increasing temperature, indicating that U(VI) surface complexation
10 reactions on edge sites are endothermic. Similar observations have been reported for
11 Eu(III)/montmorillonite and Eu(III)/kaolinite sorption systems [16].

12 In principle, the equilibrium constants deduced in this study could be considered as
13 intrinsic constants, although the electrostatic correction for clays is still a matter of
14 discussion [11, 16, 25]. To assess $\Delta_r H_m^\theta$ of the surface reactions in the model, K^{int}
15 at 298 ± 2 , 333 ± 2 and $353 \pm 2 \text{ K}$ should be first obtained. The K^{int} of surface reactions
16 at 333 ± 2 and $353 \pm 2 \text{ K}$ were obtained by fitting the SCM to the sorption data at the
17 respective temperatures. The prerequisite information for these fittings is that all
18 $\Delta_r H_m^\theta$ of the related reactions, either in the aqueous phase or at the surface, should
19 be known, because both the standard equilibrium constants at 298.15 K and the
20 $\Delta_r H_m^\theta$ of these reactions are needed to calculate the equilibration constants at
21 elevated temperatures. The $\Delta_r H_m^\theta$ of some U(VI) hydrolysis reactions were not
22 available in both the NEA [19] and the Nagra/PSI databases [20], and were assumed

1 to be 0 in calculations. This implies that the standard equilibrium constants at 298.15
2 K were used in the whole temperature range. The $\Delta_r H_m^\theta$ of surface reactions
3 responsible for the acid-base chemistry of the Na-bentonite were also assumed to be
4 0. This assumption is reasonable according to the work by Duc et al. [17], which
5 indicated that the protonation and deprotonation reactions on edge sites of
6 montmorillonite are not significantly temperature-dependent. Moreover, according to
7 the negligible temperature effect upon U(VI) sorption at low pH (Fig. 6), the $\Delta_r H_m^\theta$
8 of UO_2^{2+} binding on the layer sites was directly assumed to be 0. Similar
9 assumptions have been made for Eu(III) sorption on montmorillonite and kaolinite
10 [16]. Based on the above assumptions, the K^{int} of surface reactions (5)—(7) at 333 ± 2
11 and 353 ± 2 K were estimated by using the geochemical modeling code PHREEQC
12 [18]. The obtained K^{int} values are listed in Table 3 and the calculated results by the
13 model are presented as lines in Fig. 6. The K^{int} values of reactions (5)—(7) increase
14 with increasing temperature.

15 According to the van't Hoff equation, $\log K^{\text{int}}$ values are plotted against $1/T$, and the
16 plots for reactions (5)—(7) are illustrated in Fig. 7. Good correlation coefficients are
17 obtained in all cases, which may imply that the assumptions made above are to some
18 extent reasonable. From the slopes of these plots, $\Delta_r H_m^\theta$ of reactions (5)—(7) are
19 calculated and listed also in Table 3. The positive $\Delta_r H_m^\theta$ indicate that the surface
20 complexation reactions (5)—(7) are endothermic processes, which are consistent
21 with the experimental observations. In principle, the proposed SCM and $\Delta_r H_m^\theta$ of
22 the surface reactions may enable U(VI) sorption on the Na-bentonite at other

1 temperatures to be predicted. Finally, it should be pointed out that complementary
2 $\Delta_r H_m^\theta$ of U(VI) aqueous reactions which are not listed in the databases are
3 necessary to carry out reliable predictions of U(VI) sorption at variable temperatures.

4 **4. Conclusions**

5 Based on the experimental and modeling results in the present study, the following
6 conclusions can be made:

7 (1) U(VI) sorption on the purified Na-bentonite at different temperatures (298±2,
8 333±2 and 353±2 K) could be quantitatively described by the SCM with a complex
9 on layer sites (X_2UO_2) and three complexes on edge sites ($\equiv SOUO_2^+$,
10 $\equiv SO(UO_2)_3(OH)_5$, and $\equiv SO(UO_2)_3(OH)_7^{2-}$). It seems that the nature of the surface
11 species is governed by U(VI) speciation in solution.

12 (2) U(VI) sorption on the Na-bentonite in the presence of CO_2 ($P_{CO_2} = 10^{-3.58}$ atm) is
13 identical to that in the absence of CO_2 at pH < 6. The SCM could interpret the
14 identical sorption at pH < 6 and the lower sorption at pH > 7.5. However, it
15 underestimates to some extent the sorption of U(VI) around pH 7 in the presence of
16 CO_2 .

17 (3) The binding of UO_2^{2+} on the layer sites is apparently independent of temperature,
18 whereas the surface complexation reactions on edge sites are endothermic. The
19 $\Delta_r H_m^\theta$ of surface complexation reactions of UO_2^+ , $(UO_2)_3(OH)_5^+$, and $(UO_2)_3(OH)_7^-$
20 on the edge sites are 52, 158, and 188 kJ/mol, respectively.

Acknowledgments

The financial support by the National Natural Science Foundation of China (No. 20971061) is gratefully appreciated.

References

1. McKinley, J.P., Zachara, J.M., Smith, S.C., Turner, G.D.: The influence of uranyl hydrolysis and multiple site-binding reactions on adsorption of U(VI) to montmorillonite. *Clays Clay Miner.* **43**, 586 (1995).
2. Turner, G.D., Zachara, J.M., McKinley, J.P., Smith, S.C.: Surface-charge properties and UO_2^{2+} adsorption of a subsurface smectite. *Geochim. Cosmochim. Acta* **60**, 3399 (1996).
3. Pabalan, R.T., Turner, D.R.: Uranium (6+) sorption on montmorillonite: Experimental and surface complexation modeling study. *Aquat. Geochem.* **2**, 203 (1997).
4. Chisholm-Brause, C.J., Berg, J.M., Matzner, R.A., Morris, D.E.: Uranium(VI) Sorption Complexes on Montmorillonite as a Function of Solution Chemistry. *J. Colloid Interface Sci.* **233**, 38 (2001).
5. Greathouse, J.A., Cygan, R.T.: Water Structure and Aqueous Uranyl(VI) Adsorption Equilibria onto External Surfaces of Beidellite, Montmorillonite, and Pyrophyllite: Results from Molecular Simulations. *Environ. Sci. Technol.* **40**, 3865 (2006).
6. Kowal-Fouchard, A., Drot, R., Simoni, E., Ehrhardt, J.J.: Use of Spectroscopic Techniques for Uranium(VI)/Montmorillonite Interaction Modeling. *Environ. Sci. Technol.* **38**, 1399(2004).
7. Sylwester, E.R., Hudson, E.A., Allen, P.G.: The structure of uranium(VI) sorption complexes on silica, alumina, and montmorillonite. *Geochim. Cosmochim. Acta* **64**, 2431 (2000).
8. Catalano, J.G., Brown Jr., G.E.: Uranyl adsorption onto montmorillonite :

- Evaluation of binding sites and carbonate complexation, *Geochim. Cosmochim. Acta* **69**, 2995 (2005).
9. Korichia, S., Bensmaili, A.: Sorption of uranium (VI) on homoionic sodium smectite experimental study and surface complexation modeling, *J. Hazard. Mater.* **169**, 780 (2009).
 10. Baeyens, B., Bradbury, M.H.: A mechanistic description of Ni and Zn sorption on Na-montmorillonite Part I: Titration and sorption measurements, *J. Contam. Hydrol.* **27**, 199 (1997).
 11. Bradbury, M.H., Baeyens, B.: Sorption of Eu on Na- and Ca-montmorillonites: experimental investigations and modelling with cation exchange and surface complexation. *Geochim. Cosmochim. Acta* **66**, 2325 (2002).
 12. Kraepiel, A.M.L., Keller, K., Morel, F.M.M.: On the Acid–Base Chemistry of Permanently Charged Minerals, *Environ. Sci. Technol.* **32**, 2829 (1998).
 13. Tertre, E., Castet, S., Berger, G., Loubet, M., Giffaut, E.: Geochim. Surface chemistry of kaolinite and Na-montmorillonite in aqueous electrolyte solutions at 25 and 60 °C: Experimental and modeling study. *Geochim. Cosmochim. Acta* **70**, 4579 (2006).
 14. Guo, Z., Xu, J., Shi, K., Tang, Y., Wu, W., Tao, Z.: Eu(III) adsorption/desorption on Na-bentonite: Experimental and modeling studies. *Colloids and Surfaces A: Physicochem. Eng. Aspects* **339**, 126 (2009).
 15. Tertre, E., Berger, G., Castet, S., Loubet, M., Giffaut, E.: Experimental sorption of Ni²⁺, Cs⁺ and Ln³⁺ onto a montmorillonite up to 150 °C. *Geochim. Cosmochim. Acta* **69**, 4937 (2005).
 16. Tertre, E., Berger, G., Simoni, E., Castet, S., Giffaut, E., Loubet, M., Catalette, H. : Europium retention onto clay minerals from 25 to 150 °C: Experimental measurements, spectroscopic features and sorption modelling. *Geochim. Cosmochim. Acta* **70**, 4563 (2006).
 17. Duc, M., Carteret, C., Thomas, F., Gaboriaud, F.: Temperature effect on the acid-base behavior of Na-montmorillonite. *J. Colloid Interface Sci.* **327**, 472 (2008).

18. Parkhurst, D.L., Appelo, C.A.J.: *User's guide to PHREEQC (Version 2)—a computer program for speciation, batch-reaction, one-dimensional transport, and inverse geochemical calculations*, U.S.G.S. Water-Resources Report 99-4259, 1999.
19. Grenthe, I., Fuger, J., Konings, R., Lemire, R.J., Muller, A.B., Nguyen-Trung, C., Wanner, H.: *Chemical Thermodynamics of Uranium* (H. Wanner and I. Forest, ed.). Nuclear Energy Agency, Organisation for Economic Co-operation and Development, Elsevier, 1992.
20. Hummel, W., Berner, U., Curti, E., Pearson, F.J., Thoenen, T.: *Nagra/PSI Chemical Thermodynamic Data Base 01/01*. Universal Publishers/uPUBLISH.com USA. Also issued as Nagra Technical Report NTB 02-16, Nagra, Wettingen, Switzerland, 2002.
21. Guo, Z., Li, Y., Wu, W.: Sorption of U(VI) on goethite: Effects of pH, ionic strength, phosphate, carbonate and fulvic acid. *Appl. Radiat. Isotopes* **67**, 996 (2009).
22. Davis, J.A., Meece, D.E., Kohler, M., Curtis, G.P.: Approaches to surface complexation modeling of Uranium(VI) adsorption on aquifer sediments, *Geochim. Cosmochim. Acta* **68**, 3621 (2004).
23. Waite, T.D., Davis, J.A., Payne, T.E., Waychunas, G.A., Xu, N.: Uranium(VI) adsorption to ferrihydrite: Application of a surface complexation model. *Geochim. Cosmochim. Acta* **58**, 5465 (1994).
24. Lenhart, J.J., Honeyman, B.D.: Uranium(VI) sorption to hematite in the presence of humic acid. *Geochim. Cosmochim. Acta* **63**, 2891 (1999).
25. Montavon, G., Guo, Z., Lützenkirchen, J., Alhajji, E., Kedziorek, M.A.M., Bourg, A.C.M., Grambow, B.: Interaction of selenite with MX-80 bentonite: Effect of minor phases, pH, selenite loading, solution composition and compaction, *Colloids and Surfaces A: Physicochem. Eng. Aspects* **332**, 71 (2009).

Table 1. Modeling parameters for the acid-base chemistry of the Na-bentonite [14].

<i>Description of the purified Na-bentonite</i>	
Specific surface area	53.6 m ² /g
<i>Sites</i>	<i>Site density</i>
X ⁻	1.16×10 ⁻⁵ mol/m ² (623 meq/kg)
≡SOH	5.88×10 ⁻⁷ mol/m ²
≡YOH	1.18×10 ⁻⁶ mol/m ²
<i>Aqueous solution/solid equilibria: Reactions involved in acid-base titration</i>	
Reactions	logK ^{int} (T = 298 K)
XNa \rightleftharpoons X ⁻ + Na ⁺	-1.3
XNa + H ⁺ \rightleftharpoons XH + Na ⁺	0.79
≡SOH + H ⁺ \rightleftharpoons ≡SOH ₂ ⁺	3.23
≡SOH \rightleftharpoons ≡SO ⁻ + H ⁺	-3.89
≡YOH \rightleftharpoons ≡YO ⁻ + H ⁺	-6.57

Table 2. Thermodynamic data for aqueous reactions of U(VI) used in modeling ($I = 0$, $T = 298.15\text{K}$) [19, 20].

Reactions	logK	$\Delta_r H_m^\circ$ (kJ/mol)
$\text{UO}_2^{2+} + \text{H}_2\text{O} \rightleftharpoons \text{UO}_2\text{OH}^+ + \text{H}^+$	-5.20	58
$\text{UO}_2^{2+} + 2\text{H}_2\text{O} \rightleftharpoons \text{UO}_2(\text{OH})_2(\text{aq}) + 2\text{H}^+$	-12.0	20
$\text{UO}_2^{2+} + 3\text{H}_2\text{O} \rightleftharpoons \text{UO}_2(\text{OH})_3^- + 3\text{H}^+$	-19.2	—
$\text{UO}_2^{2+} + 4\text{H}_2\text{O} \rightleftharpoons \text{UO}_2(\text{OH})_4^{2-} + 4\text{H}^+$	-33.0	—
$2\text{UO}_2^{2+} + \text{H}_2\text{O} \rightleftharpoons (\text{UO}_2)_2\text{OH}^{3+} + \text{H}^+$	-2.70	—
$2\text{UO}_2^{2+} + 2\text{H}_2\text{O} \rightleftharpoons (\text{UO}_2)_2(\text{OH})_2^{2+} + 2\text{H}^+$	-5.62	54
$3\text{UO}_2^{2+} + 4\text{H}_2\text{O} \rightleftharpoons (\text{UO}_2)_3(\text{OH})_4^{2+} + 4\text{H}^+$	-11.9	—
$3\text{UO}_2^{2+} + 5\text{H}_2\text{O} \rightleftharpoons (\text{UO}_2)_3(\text{OH})_5^+ + 5\text{H}^+$	-15.55	105
$3\text{UO}_2^{2+} + 7\text{H}_2\text{O} \rightleftharpoons (\text{UO}_2)_3(\text{OH})_7^- + 7\text{H}^+$	-31.0	—
$4\text{UO}_2^{2+} + 7\text{H}_2\text{O} \rightleftharpoons (\text{UO}_2)_4(\text{OH})_7^+ + 7\text{H}^+$	-21.9	—
$\text{UO}_2^{2+} + \text{CO}_3^{2-} \rightleftharpoons \text{UO}_2\text{CO}_3(\text{aq})$	9.68	5.0
$\text{UO}_2^{2+} + 2\text{CO}_3^{2-} \rightleftharpoons \text{UO}_2(\text{CO}_3)_2^{2-}$	16.94	18.5
$\text{UO}_2^{2+} + 3\text{CO}_3^{2-} \rightleftharpoons \text{UO}_2(\text{CO}_3)_3^{4-}$	21.60	-39.2
$3\text{UO}_2^{2+} + 6\text{CO}_3^{2-} \rightleftharpoons (\text{UO}_2)_3(\text{CO}_3)_6^{6-}$	54.00	-62.7
$2\text{UO}_2^{2+} + \text{CO}_2(\text{g}) + 4\text{H}_2\text{O}(\text{l}) \rightleftharpoons (\text{UO}_2)_2\text{CO}_3(\text{OH})_3^- + 5\text{H}^+$	-19.01	—
$3\text{UO}_2^{2+} + \text{CO}_2(\text{g}) + 4\text{H}_2\text{O}(\text{l}) \rightleftharpoons (\text{UO}_2)_3\text{O}(\text{OH})_2(\text{HCO}_3)^+ + 5\text{H}^+$	-17.5	—
$11\text{UO}_2^{2+} + 6\text{CO}_2(\text{g}) + 18\text{H}_2\text{O}(\text{l}) \rightleftharpoons (\text{UO}_2)_{11}(\text{CO}_3)_6(\text{OH})_{12}^{2-} + 24\text{H}^+$	-72.5	—
$\text{UO}_2^{2+} + \text{Cl}^- \rightleftharpoons \text{UO}_2\text{Cl}^+$	0.17	8.0
$\text{UO}_2^{2+} + 2\text{Cl}^- \rightleftharpoons \text{UO}_2\text{Cl}_2(\text{aq})$	-1.10	15

Table 3. Surface complexation reactions of U(VI) on Na-bentonite and corresponding intrinsic equilibrium constants ($I = 0$ mol/L).

U(VI) surface complexation reactions	$\log K^{int}$			$\Delta_r H_m^\theta$ (kJ/mol)
	298±2 K	333±2 K	353±2 K	
$2XNa + UO_2^{2+} \rightleftharpoons X_2(UO_2)_2 + 2Na^+$	0.6	0.6	0.6	0
$\equiv SOH + UO_2^{2+} \rightleftharpoons \equiv SOUO_2^+ + H^+$	-0.9	0.1	0.5	52
$\equiv SOH + 3UO_2^{2+} + 5H_2O \rightleftharpoons \equiv SO(UO_2)_3(OH)_5 + 6H^+$	-15.7	-13.1	-11.3	158
$\equiv SOH + 3UO_2^{2+} + 7H_2O \rightleftharpoons \equiv SO(UO_2)_3(OH)_7^{2-} + 8H^+$	-26.2	-23.0	-21.0	188

Figure Captions

Fig. 1. Sorption curves of U(VI) versus pH on the Na-bentonite at different initial U(VI) concentrations; $T = 298 \pm 2$ K, $I = 0.1$ mol/L NaCl and $m/V = 1$ g/L. The points show the experimental data and the solid lines represent the results calculated by the proposed model. The dash lines illustrate the contributions of different surface complexes to U(VI) sorption at $C_{U(VI)}^0 = 8.02 \times 10^{-5}$ mol/L: (A) X_2UO_2 ; (B) $\equiv SOUO_2^+$; (C) $\equiv SO(UO_2)_3(OH)_5$; (D) $\equiv SO(UO_2)_3(OH)_7^{2-}$.

Fig. 2. Speciation of U(VI) in NaCl solution; $T = 298.15$ K, $C_{U(VI)}^0 = 4.0 \times 10^{-5}$ mol/L and $I = 0.1$ mol/L NaCl; (a) $P_{CO_2} = 0$; (b) $P_{CO_2} = 10^{-3.58}$ atm; Solids are not allowed to precipitate.

Fig. 3. Sorption isotherms of U(VI) on the Na-bentonite; $T = 298 \pm 2$ K, $I = 0.1$ mol/L NaCl and $m/V = 1$ g/L. The points show the experimental data and the lines represent the results calculated by the proposed model.

Fig. 4. Effect of m/V upon U(VI) sorption on the Na-bentonite; $T = 298 \pm 2$ K, $C_{U(VI)}^0 = 8.02 \times 10^{-5}$ mol/L, $pH = 5.00 \pm 0.10$ and $I = 0.1$ mol/L NaCl. The points show the experimental data and the line represents the results calculated by the proposed model.

Fig. 5. Sorption curves of U(VI) versus pH on the Na-bentonite in the presence and absence of CO_2 ; $T = 298 \pm 2$ K, $C_{U(VI)}^0 = 8.02 \times 10^{-5}$ mol/L, $I = 0.1$ mol/L NaCl and $m/V = 1$ g/L. The points show the experimental data, the solid line represents the results calculated by the proposed model for the sorption system at $P_{CO_2} = 10^{-3.58}$ atm. The dash lines illustrate the contributions of different surface complexes to U(VI) sorption at $P_{CO_2} = 10^{-3.58}$ atm: (A) X_2UO_2 ; (B) $\equiv SOUO_2^+$; (C) $\equiv SO(UO_2)_3(OH)_5$; (D) $\equiv SO(UO_2)_3(OH)_7^{2-}$.

Fig. 6. Sorption curves of U(VI) versus pH on the Na-bentonite at different

temperatures; $C_{\text{U(VI)}}^0 = 8.02 \times 10^{-5} \text{ mol/L}$, $I = 0.1 \text{ mol/L NaCl}$, $m/V = 1 \text{ g/L}$.

The points show the experimental data and the lines represent the results calculated by the proposed model with the equilibrium constants listed in Table 3.

Fig. 7. The dependence of equilibrium constants (K^{int}) of U(VI) surface complexation reactions on temperature according to the van't Hoff equation; (a) $\equiv\text{SOUO}_2^+$; (b) $\equiv\text{SO}(\text{UO}_2)_3(\text{OH})_5$; (c) $\equiv\text{SO}(\text{UO}_2)_3(\text{OH})_7^{2-}$.

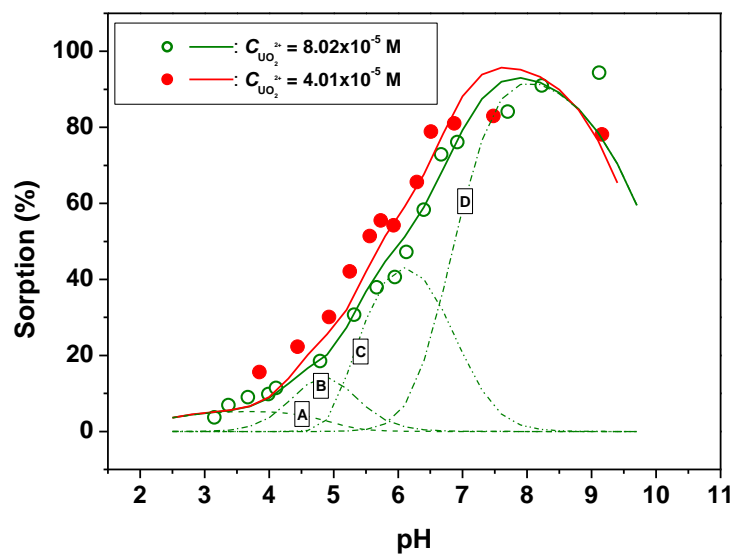


Fig. 1. Sorption curves of U(VI) versus pH on the Na-bentonite at different initial U(VI) concentrations; $T = 298 \pm 2$ K, $I = 0.1$ mol/L NaCl and $m/V = 1$ g/L. The points show the experimental data and the solid lines represent the results calculated by the proposed model. The dash lines illustrate the contributions of different surface complexes to U(VI) sorption at $C_{U(VI)}^0 = 8.02 \times 10^{-5}$ mol/L: (A) X_2UO_2 ; (B) $\equiv SOUO_2^+$; (C) $\equiv SO(UO_2)_3(OH)_5$; (D) $\equiv SO(UO_2)_3(OH)_7^{2-}$.

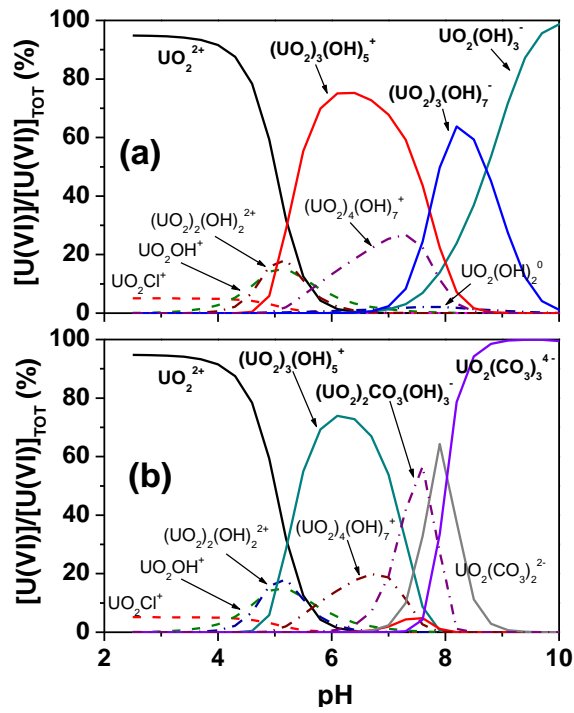


Fig. 2. Speciation of U(VI) in NaCl solution; $T = 298.15\text{K}$, $C_{U(VI)}^0 = 4.0 \times 10^{-5} \text{ mol/L}$ and $I = 0.1 \text{ mol/L NaCl}$; (a) $P_{CO_2} = 0$; (b) $P_{CO_2} = 10^{-3.58} \text{ atm}$; Solids are not allowed to precipitate.

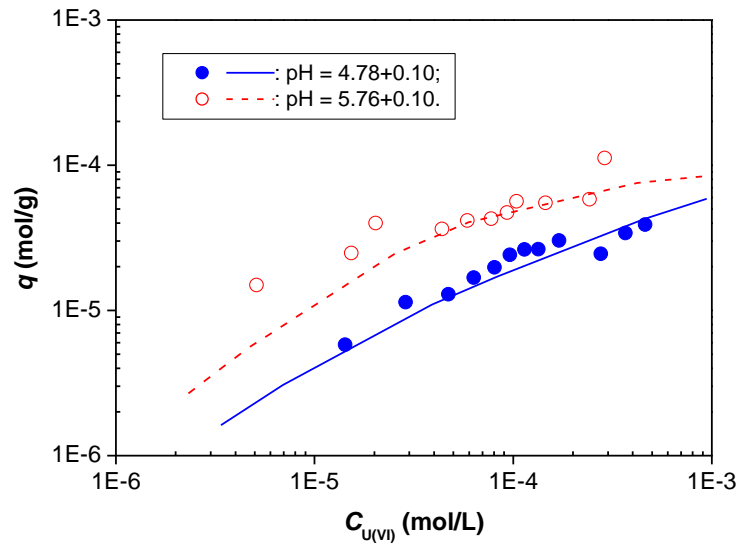


Fig. 3. Sorption isotherms of U(VI) on the Na-bentonite; $T = 298 \pm 2$ K, $I = 0.1$ mol/L NaCl and $m/V = 1$ g/L. The points show the experimental data and the lines represent the results calculated by the proposed model.

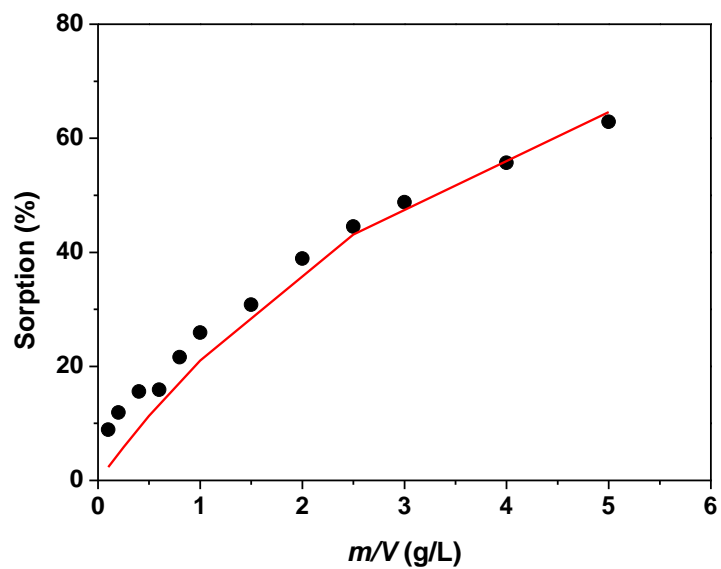


Fig. 4. Effect of m/V upon U(VI) sorption on the Na-bentonite; $T = 298 \pm 2$ K, $C_{\text{U(VI)}}^0 = 8.02 \times 10^{-5}$ mol/L, $\text{pH} = 5.00 \pm 0.10$ and $I = 0.1$ mol/L NaCl. The points show the experimental data and the line represents the results calculated by the proposed model.

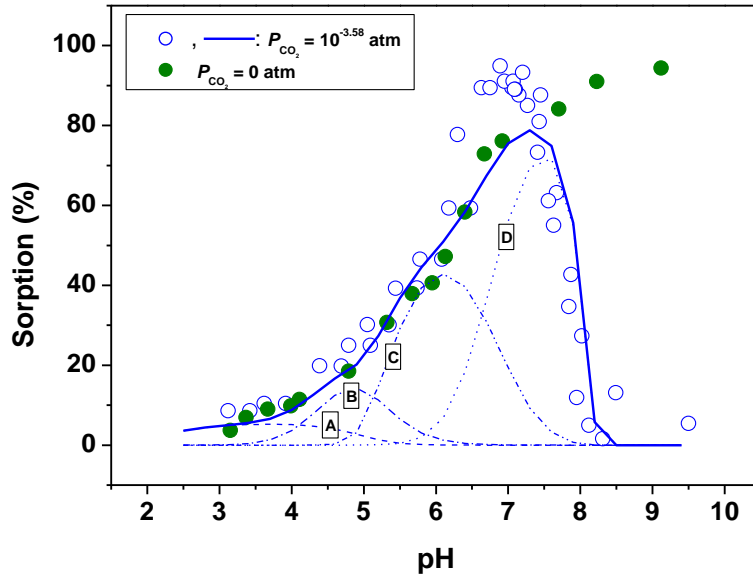


Fig. 5. Sorption curves of U(VI) versus pH on the Na-bentonite in the presence and absence of CO₂; $T = 298 \pm 2$ K, $C_{U(VI)}^0 = 8.02 \times 10^{-5}$ mol/L, $I = 0.1$ mol/L NaCl and $m/V = 1$ g/L. The points show the experimental data, the solid line represents the results calculated by the proposed model for the sorption system at $P_{CO_2} = 10^{-3.58}$ atm. The dash lines illustrate the contributions of different surface complexes to U(VI) sorption at $P_{CO_2} = 10^{-3.58}$ atm: (A) X_2UO_2 ; (B) $\equiv SOUO_2^+$; (C) $\equiv SO(UO_2)_3(OH)_5$; (D) $\equiv SO(UO_2)_3(OH)_7^{2-}$.

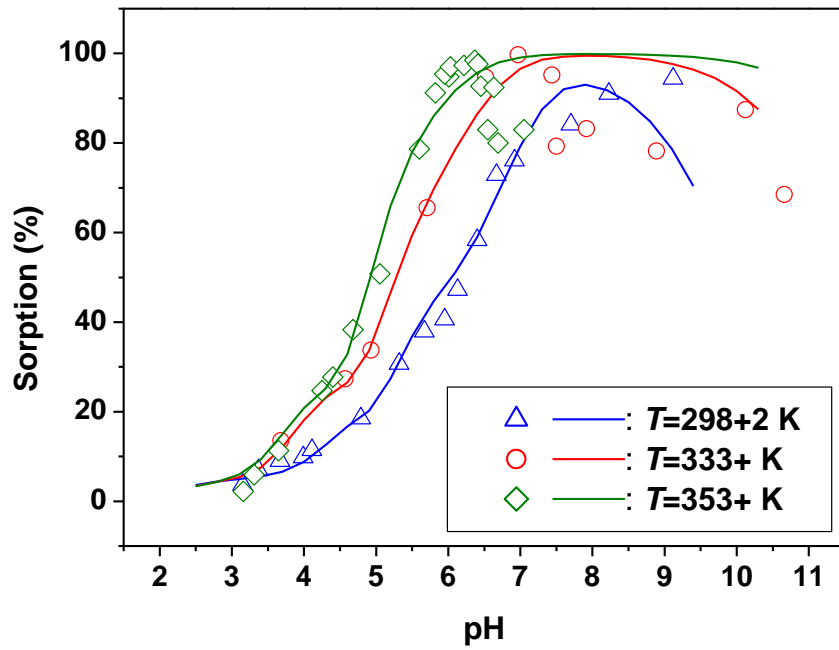


Fig. 6. Sorption curves of U(VI) versus pH on the Na-bentonite at different temperatures; $C_{U(VI)}^0 = 8.02 \times 10^{-5}$ mol/L, $I = 0.1$ mol/L NaCl, $m/V = 1$ g/L. The points show the experimental data and the lines represent the results calculated by the proposed model with the equilibrium constants listed in Table 3.

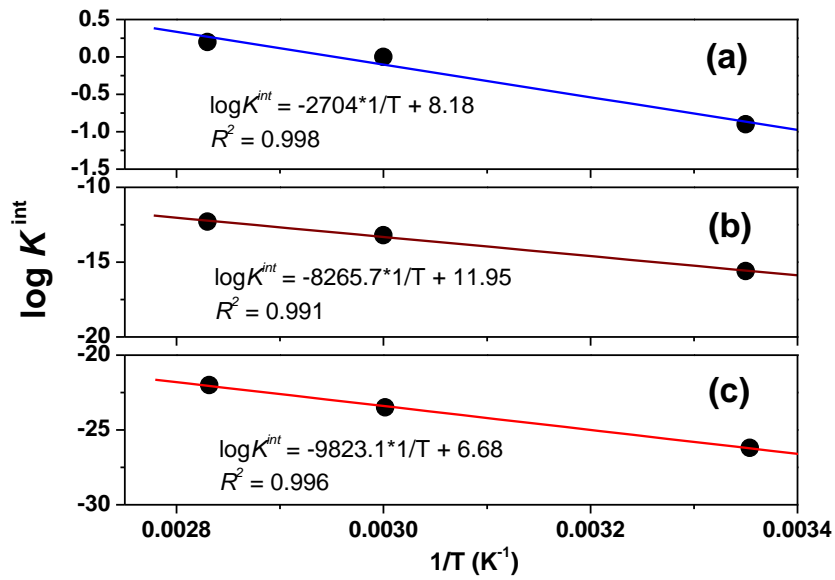


Fig. 7. The dependence of equilibrium constants (K^{int}) of U(VI) surface complexation reactions on temperature according to the van't Hoff equation; (a) $\equiv\text{SO}\text{UO}_2^+$; (b) $\equiv\text{SO}(\text{UO}_2)_3(\text{OH})_5$; (c) $\equiv\text{SO}(\text{UO}_2)_3(\text{OH})_7^{2-}$.